Shahrood University of Technology

Journal of Mining and Environment (JME)

Journal homepage: www.jme.shahroodut.ac.ir

Iranian Society of Mining Engineering (IRSME)

Assessment of Strength and Permeability Behavior of Glass Fibre-reinforced Fly Ash-Bentonite Mixture

Swaraj Chowdhury*, Rakesh Kumar, and Ankit Kumar

Department of Civil Engineering, National Institute of Technology Hamirpur, Himachal Pradesh - 177005, India

Article Info

Received 27 July 2025
Received in Revised form 28 August 2025
Accepted 7 September 2025
Published online 7 September 2025

DOI: 10.22044/jme.2025.16576.3242

Keywords

Fly ash
Bentonite, Glass fibre
Unconfined compressive strength
Coefficient of permeability

Abstract

The present study examines the strength and permeability behavior of glass fibre-reinforced fly ash-bentonite (FaB) mixture to assess its potential as an alternate geo-material. The FaB mixture is produced by adding 20% bentonite with 80% fly ash and is further reinforced with glass fibre. The unconfined compressive strength (UCS) tests have been conducted at a strain rate of 0.625 mm/min by varying the curing period (0 to 60 days), relative moisture content (R.M.C– 80% to 120%) and fibre content (0% to 1.0%). The effect of fibre content on the coefficient of permeability (k) and compressibility behavior of the FaB mixture has been investigated through one-dimensional consolidation tests. The findings indicate that the UCS of the FaB mix samples improves with an increase in curing period and fibre content. At 100% R.M.C, the UCS increases from 48 kPa to 228 kPa for the unreinforced samples as the curing period increases from 0 to 60 days. At 90% R.M.C, both unreinforced and reinforced FaB mix samples have exhibited the highest UCS values considering all curing periods. With fibre content increasing from 0% to 1.0%, the UCS rises about 33% to 44% at 100% R.M.C. Fibre reinforcement also contributes to reduction of k and compressibility. Based on the experimental findings, a closed-form equation has been developed for the prediction of UCS of FaB mixture reinforced with and without glass fibre. Results confirm that glass fibre reinforcement improves the strength, permeability, and compressibility of the FaB mixture, establishing it as an alternate geo-material.

1. Introduction

Fly ash, a by-product generated from coal combustion in thermal power plants, needs to be utilized to reduce its disposal problems. One acre of land is required to dispose the fly ash generated for electricity production of one megawatt [1]. In India, thermal power plants meet approximately 73% of electricity demand; around 300 million tons of fly ash are generated annually from these plants. This gigantic volume of ash needs over 40,000 acres of land for disposal as per the Central Electricity Authority [2], leading to the occupation of vast areas of land as “Ash ponds”. The current utilization rate of fly ash in India is approximately 78.14%, according to the CEA [2]. Despite this significant usage, a substantial quantity of fly ash remains unutilized every year. Previously researchers observed that fly/pond ash can be utilized in various geotechnical applications [3-12]. Rout and Singh [4] observed that compacted pond ash-bentonite mixes exhibit higher strength as liner than sand-bentonite mixes. Nayak et al. [6] reported about the necessity of high fly ash utilization for sustainable development. Fly/pond ash can also be utilised as partial replacement of river sand and natural aggregates, promoting resource conservation, environmental sustainability, and improved public health [8, 11]. Engineering properties of fly/pond ash can be improved through methods such as densification, stabilization, and reinforcement [13-24]. Addition of fibres in pond ash-bentonite and sand-bentonite mixtures increase their respective UCS about 2 to 3 times [14]. The static and cyclic behavior of pond ash samples improve significantly due to geogrid

Corresponding author: swaraj@nith.ac.in (S. Chowdhury)

[15] and geocell [17] reinforcement. Kedar and Patel [20] demonstrate that stabilized fly ash could be an effective replacement for granular base layer. Like fly/pond ash geogrid reinforcement can also be effective in improving the failure mechanism of concrete [23, 24]. The pozzolanic characteristics of fly ash can contribute to strength and durability improvement when mixed with weak soils [25-27]. Fly ash serves as a viable substitute for conventional geo-materials in various geotechnical applications [28], underlining its vast potential for wider utilization.

Bentonite is a commercially available clay that has been extensively utilized to reduce the permeability of backfill materials for retaining walls [29-30]. Mixing bentonite with fly ash or pond ash enhances their geotechnical properties [4, 31-32], making bentonite a viable option for the large-scale utilization of these industrial by-products. Such mixtures have shown potential as liner materials due to their low hydraulic conductivity, high adsorption capacity, and improved mechanical strength [33, 4, 29, 34-35]. Further improvements in the geotechnical behavior of the FaB mixture can be achieved by reinforcing them with various types of fibres. Fibre addition enhances the mechanical and shear strength characteristics of ash-bentonite mixture [14]. Several earlier studies have recognized the positive influence of fibre reinforcement on the engineering properties of different geo-materials [36-48]. Kumar et al. [36] show that inclusion of fibre in pond ash and silty sand increases the peak compressive strength, CBR value, peak friction angle, and ductility. Addition of fibre elements increases the liquefaction potential of fly ash [38]; it also enhances the piping resistance of fly ash and delays the attenuation of piping phenomena considerably [41]. Sun et al. [47] observed that the hybrid concrete samples containing steel fibres show higher compressive strength compared to the samples containing macro synthetic and polypropylene fibre. Fu et al. [48] investigate the effect of various fibres on the strength and flexibility of concrete. Also, several investigations have explored the influence of fibre reinforcement on both cohesive and cohesionless soils [49-57]. Maher and Gray [49] observed improvement in the shear strength behavior of sands reinforced with randomly distributed fibres. Reinforced soil with aligned and randomly oriented metallic fibres have shown significant increase in the peak and residual strengths [50]. Mukherjee and Mishra [55] explored that the compressibility, hydraulic and shrinkage behavior of the sand-bentonite mixture has been improved significantly due to the presence of the fibre. Karki and Kolay [57] observed that recycled glass powder and polypropylene fibre have strong potential for enhancing the performance highly expansive bentonite clay, offering a promising solution for construction challenges associated with expansive soils.

The rising volume of fly ash production presents both environmental challenges and opportunities for sustainable development. Utilization of fly ash for productive purposes offers a sustainable solution by mitigating disposal issues and easing the demand for high-quality granular materials. The critical review of the literature shows that there exists a limited number of studies focused on the strength and permeability behavior of ash-bentonite mixtures with and without fibre reinforcement [58, 14, 31, 35, 59-60]. Very few studies focused on the behavior of glass fibre-reinforced sand-bentonite mixture as an alternate geo-material [55-56, 61-62]. However, none of these studies have exclusively addressed the hydro-mechanical behavior of fly ash-bentonite mixtures reinforced with glass fibres. The present study aims to bridge this research gap by investigating the performance of a glass fibre-reinforced FaB mixture as an alternate geo-material, based on strength and permeability parameters. This approach offers a pathway towards sustainability by addressing the reuse of industrial by-products like fly ash and minimizing its disposal problems. The objectives of this study are as follows:

- To examine the influence of curing periods (0, 7, 14, 28, and 60 days) on the compressive strength behavior of fibre-reinforced and unreinforced FaB mixtures.
- The influence of relative moisture content (R.M.C- 80%, 90%, 100%, 110%, and 120%) on the UCS of both reinforced and unreinforced FaB mix samples has been evaluated.
- To observe the influence of varying fibre contents (0%, 0.25%, 0.5%, 0.75%, and 1%) on the UCS of FaB mix samples.
- To study the influence of glass fibre addition on the coefficient of permeability (k) and compressibility characteristics of FaB mixtures.
- To develop a closed-form equation for practitioners to predict the UCS of FaB mixtures with and without glass fibre reinforcement based on the experimental outcomes.

2. Materials & Methodology

2.1. Materials

2.1.1. Fly Ash and Bentonite

Fly ash (Fa) (Figure 1a) has been collected from the Guru Gobind Singh Super Thermal Power Plant located in Ropar, Punjab, India. The collected samples have been thoroughly homogenized, sieved through a 475 µm mesh to remove foreign and organic matter, and subsequently oven-dried at a temperature range of 105–110°C. Bentonite (Figure 1b) is a commercially available clay known for its high-water absorption and swelling characteristics due to the presence of montmorillonite. These properties make bentonite particularly effective as a liner material and stabilizer for weak soils. The FaB mixtures have been prepared by mixing 80% fly ash with 20% bentonite by dry weight. This proportion has been chosen based on the findings of Rout and Singh [4, 31, 63]; they proved that 20% bentonite content is adequate for sealing the pores of an ash material and ensures a balanced mix. Furthermore, the FaB mixture has been reinforced with glass fibre (Figure 1c) at varying contents of 0%, 0.25%, 0.5%, 0.75%, and 1% by dry weight. Figure 1(d) shows the scanning electron microscope (SEM) image of the glass fibre-reinforced FaB mix sample.

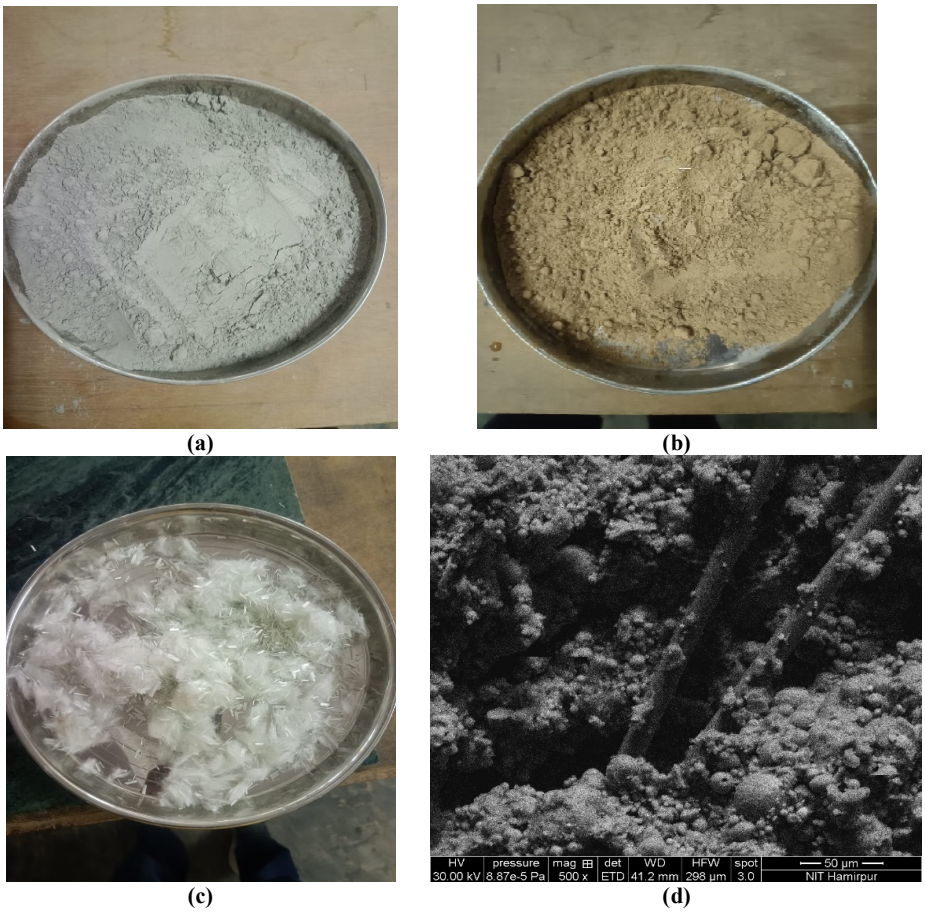

Figure 1. (a) Fly ash (b) bentonite (c) shredded glass fibre (6 mm) (d) SEM image of glass fibre-reinforced FaB mix sample

2.1.2. Glass Fibre

Glass fiber is a lightweight, durable, high-strength, low-thermal-conductivity and good chemical-resistance material. The use of glass fibres in construction has been practiced for several decades. These fibres function as binders, contributing to the strength, sustainability, and durability of soils and soil-like material [37, 40, 55-56, 61-62, 64-65]. In the present study, glass fibre is used to reinforce FaB mixtures. Glass fibre consists of composition of oxygen (54.6%), silica (21%), Alumina (6.7%), and calcium oxide (15.3%) [55]. To ensure a uniform mix with fly ash and bentonite, the fibre has been bought at a length 6 mm (Figure 1c). The fibre has been added into the FaB mixture based on the dry weight

percentage of the mixture at varying proportions, i.e., 0%, 0.25%, 0.5%, 0.75%, and 1.0%. Accordingly, the mixtures have been designated as FaB+0%G.F (unreinforced), FaB+0.25%G.F, FaB+0.5%G.F, FaB+0.75%G.F, and FaB+1%G.F, where the numerical values represent the respective percentages of glass fibre added.

2.2. Methodology

The FaB mixture has been prepared by mixing 80% fly ash with 20% bentonite, following the recommendations of Rout and Singh [63, 4, 31]. The specific gravity (G) of the 80%-20% FaB mixture has been determined using a density bottle in accordance with IS: 2720 (Part III) [66]. Particle size distribution analyses for both the fly ash and the 80%-20% FaB mixture have been conducted following the procedure outlined in IS: 2720 (Part IV) [67]. The liquid limit of the FaB mixture has been determined as per IS: 2720 (Part V) [68]. Standard Proctor compaction tests have been carried out in accordance with IS: 2720 (Part VII) [69] to determine the maximum dry density (MDD) and optimum moisture content (OMC) of the mixture. A series of unconfined compressive strength (UCS) tests have been conducted on FaB mix samples, both unreinforced and reinforced with glass fibres, with varying curing periods and R.M.C, following the IS: 2720 (Part X) [70] procedure. The wet mixture of fly ash and bentonite has been stored for 24 hours to achieve moisture equilibrium before sample preparation. Cylindrical specimens with a diameter of 38 mm and height of 76 mm have been prepared using a static compactor at relative moisture contents ranging from 80% to 120%. Relative moisture content (R.M.C) refers to the ratio of molding water content to the OMC, expressed as a percentage. The selected R.M.Cs are 80%, 90%, 100%, 110%, and 120%, which signify OMC−4%, OMC−2%, OMC, OMC+2%, and OMC+4%, respectively. The required quantities of water, fly ash, and bentonite for sample preparation have been determined based on the specified R.M.C and corresponding dry densities. For reinforced specimens, varying amounts of glass fibre (0%, 0.25%, 0.5%, 0.75%, and 1.0%) have been added into the FaB mixture. All the UCS specimens have been cured at a temperature of 27±1°C for different time periods of 0, 7, 14, 28, and 60 days, under film-wrapped conditions to prevent moisture loss. The cured specimens have been tested using a strain-controlled unconfined compression testing machine operating at a strain rate of 0.625 mm/min. The UCS values have been derived from the axial stress–axial strain curves obtained from testing. Figure 2(a) shows the FaB mix sample before testing and Figure 2(b) shows the micro cracks and propagation of the failure plane during UCS testing. The observed crack-propagation mechanism has a similarity with the observations by previous researchers [71-75]. The one-dimensional consolidation tests have been carried out in an oedometer in accordance with the IS: 2720 (Part XV) –1986 [76] procedure, as shown in Figure 2(c), to assess the compressibility and coefficient of permeability of compacted FaB mixtures containing varying amounts of glass fibres. The test specimens, each 60 mm in diameter and 20 mm in height, have been statically compacted to their respective MDD and OMC. For reinforced specimens, glass fibre has been mixed with the FaB mixture at varying contents (0%, 0.25%, 0.5%, 0.75%, and 1.0%).

3. Results and Discussion

3.1. Basic Geotechnical Properties

The specific gravity and liquid limit of the FaB mixture have been determined as 2.2 and 55.6%, respectively. The particle size distribution curve (Figure 3) of the fly ash and FaB mixture has been obtained through sieve and hydrometer analyses. The coefficient of uniformity and coefficient of curvature for the fly ash and FaB mixture are 2.2, 1.16 and 6.66, 3.26, respectively. The compaction behavior of the mixture has been evaluated using the standard Proctor compaction test to determine the OMC and MDD. The MDD and OMC of the FaB mixture have been found to be 13.94 kN/m³ and 19.8%, respectively.

(a)

(b)

(c)

Figure 2. (a) FaB mix sample before testing (b) Propagation of failure plane during UCS testing (c) One-dimensional consolidation testing

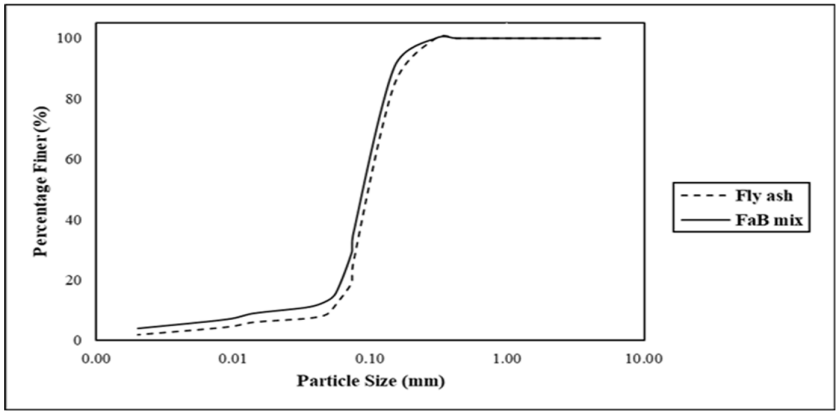

Figure 3. Particle size distribution curve for fly ash and FaB mix

3.2. Unconfined Compressive Strength (UCS)

3.2.1. Influence of Curing Period on UCS

The curing period significantly influences the strength development of the unreinforced and glass fibre-reinforced FaB mix samples. Figure 4 (a-e) shows the influence of the curing period on the axial stress–axial strain behavior of these samples. As the curing period varies from 0 to 60 days, the UCS values of both reinforced and unreinforced FaB mix samples increase. For unreinforced FaB mix samples, the UCS rises from 48 kPa to 228 kPa, whereas for FaB+1%G.F mix samples, it

increases from 71 kPa to 329 kPa. As curing period rises beyond 7 days, the failure pattern for both unreinforced and glass fibre-reinforced FaB mix samples becomes more brittle. As shown in Figure 5, with an increase in curing time from 0 to 60 days, the UCS rises from 48 kPa to 228 kPa for FaB+0%G.F, 47 kPa to 239 kPa for FaB+0.25%G.F, 66 kPa to 253 kPa for FaB+0.5%G.F, 66 kPa to 271 kPa for FaB+0.75%G.F, and 71 kPa to 329 kPa for FaB+1%G.F mix samples. The reason behind this improvement in UCS is the high-water absorption capacity of bentonite that allows it to hydrate over time, facilitating prolonged pozzolanic activity within the FaB mixture. The hydrated bentonite improves particle cohesion, while the formation of cementitious compounds, which gradually fills voids and micro-cracks, resulting in densification. The densification of the mixture enhances the overall strength of FaB mix samples as curing time progresses.

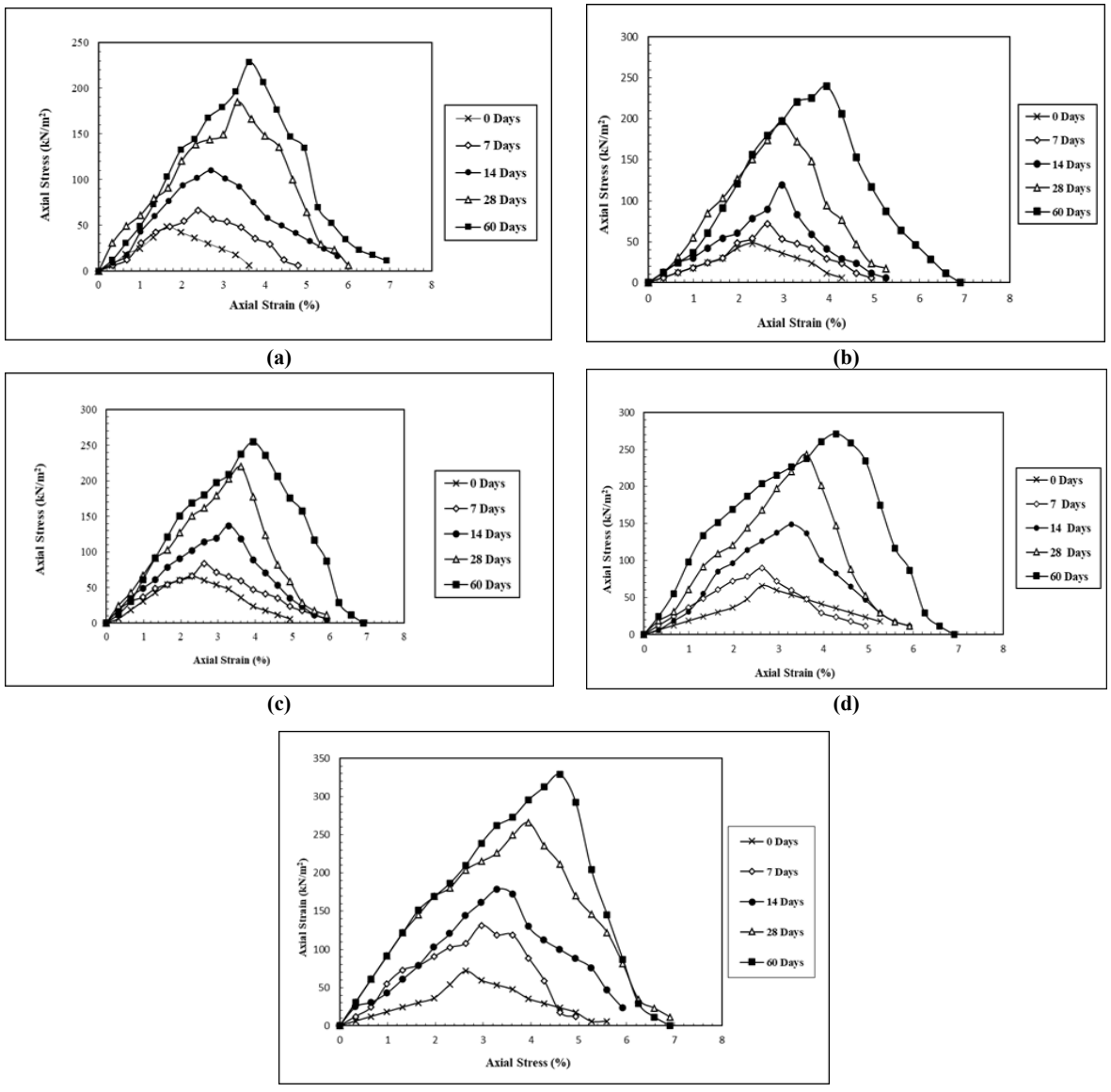

Figure 4. Axial stress – axial strain behavior with varying curing periods for (a) FaB+0%G.F (unreinforced) mix (b) FaB+0.25%G.F mix (c) FaB+0.5%G.F mix (d) FaB+0.75%G.F mix (e) FaB+1%G.F mix

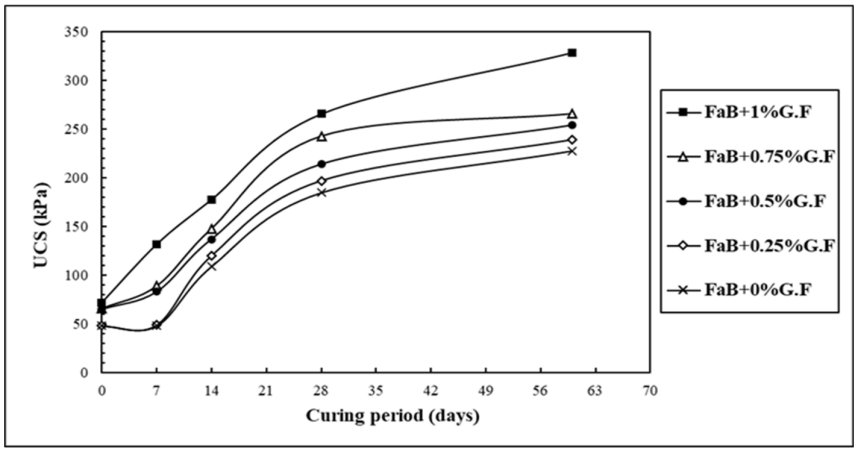

Figure 5. Variation of UCS for unreinforced and reinforced FaB mix samples with varying curing periods

3.2.2. Influence of Relative Moisture Content (R.M.C) on UCS

The relative moisture content (R.M.C) of FaB mix samples significantly influences their axial stress–axial strain behavior and UCS values. To investigate the influence of R.M.C on the UCS of unreinforced and glass fibre-reinforced FaB mix samples, cylindrical UCS specimens have been prepared at varying R.M.C- 80%, 90%, 100%, 110%, and 120% (R.M.C calculation is provided in Section 2.2). Figure 6(a–b) illustrate the axial stress–axial strain behavior of unreinforced FaB mix samples at different R.M.C after 28 and 60 days of curing, respectively. Correspondingly, Figure 7(a–b) depicts the same behavior for FaB+1%G.F mix samples with respect to the same R.M.C and curing periods. The results indicate that R.M.C significantly influences the axial stress–axial strain behavior for both unreinforced and reinforced FaB mix samples. Irrespective of the curing period, the peak axial stress for both types of samples has been observed at 90% R.M.C. At 28 days of curing, the UCS values have been recorded as 160 kPa, 229 kPa, 185 kPa, 147 kPa, and 112 kPa for unreinforced samples and 230 kPa, 302 kPa, 278 kPa, 201 kPa, and 147 kPa for 1% glass fibre-reinforced samples, corresponding to R.M.C of 80%, 90%, 100%, 110%, and 120%, respectively. Figure 8(a–b) shows the UCS variation with R.M.C for unreinforced and reinforced FaB mix samples. It has been observed that UCS increases as R.M.C increases from 80% to 90% across all curing periods. This is because the additional water enhances pozzolanic reactions, leading to a stronger matrix and thus improving strength. Also, at 90% R.M.C, water provides an optimal lubricating effect, enabling denser particle rearrangement during static compaction. Beyond 90% R.M.C, the UCS values gradually decrease, regardless of curing duration and reinforcement condition. Excess water beyond this point (90% R.M.C) leads to an increase in lubrication, which weakens the interfacial interactions between particles and between fibres and particles. This results in slippage of cohesive particles and pulling out of fibres before fully mobilizing their tensile strength, ultimately reducing the overall strength.

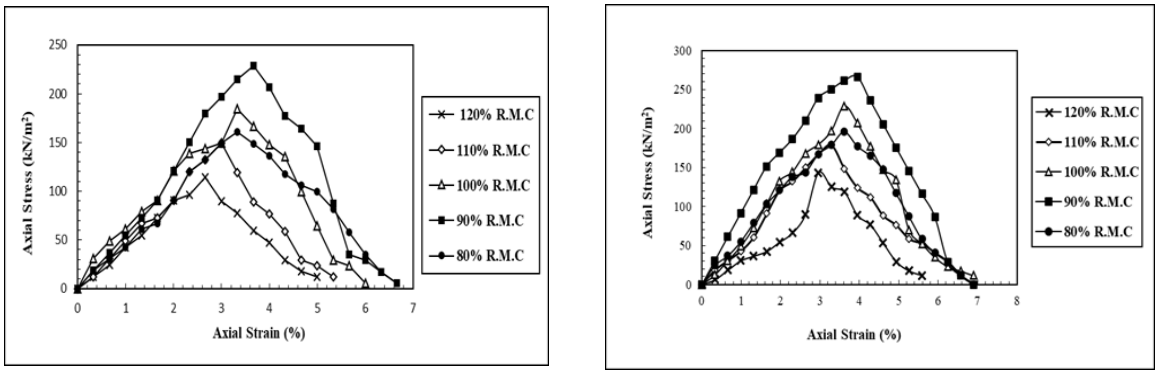

(a) **(b)**

Figure 6. Axial stress – axial strain behavior for FaB+0%G.F (unreinforced) mix sample at (a) 28 days and (b) 60 days curing period

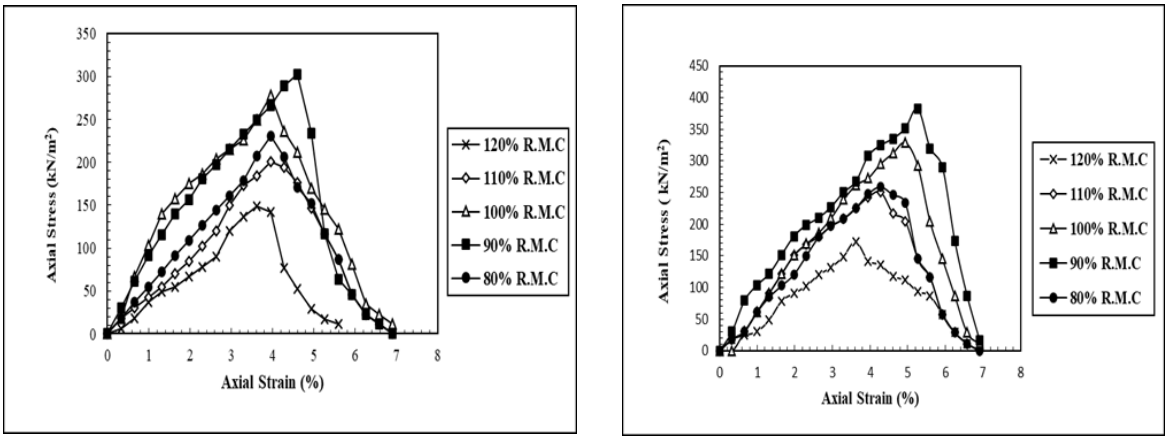

(a) (b)

Figure 7. Axial stress – axial strain behavior for FaB+1%G.F mix sample at (a) 28 days and (b) 60 days curing period

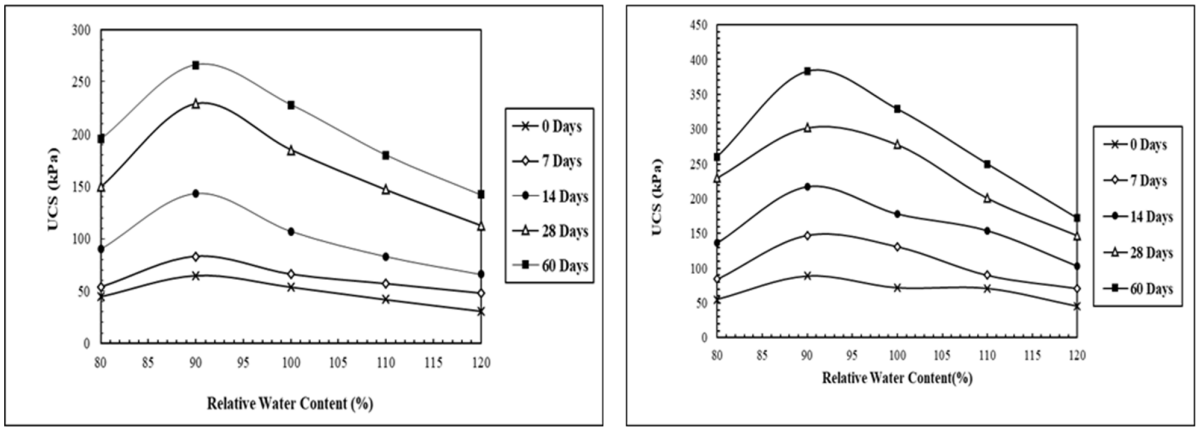

(a) (b)

Figure 8. Variation of UCS with R.M.C for (a) FaB+0%G.F (unreinforced) mix and (b) FaB+1%G.F mix samples

3.2.3. Influence of Glass Fibre Content on UCS

The fibre content plays a significant role in enhancing the axial stress–axial strain behavior and the UCS of FaB mix samples. To observe the influence of fibre content on the UCS of FaB mix samples, UCS specimens have been prepared with varying fibre contents (0%, 0.25%, 0.5%, 0.75%, and 1%). Figure 9 (a–c) show the axial stress–axial strain behavior of FaB mix samples with different fibre contents after 7, 28, and 60 days of curing period. It is evident that the peak stress increases with higher fibre content across all curing periods.

Figure 10 shows the variation in UCS values with varying fibre content. It is observed that the UCS of FaB mix samples increases as the fibre content increases from 0% to 1%; the UCS rises from 60 kPa to 132 kPa, 185 kPa to 266 kPa, and 228 kPa to 329 kPa after 7, 28, and 60 days of curing time period. The increase in UCS with higher fibre content is attributed to the mechanical interactions between the fibres and the fly ash and bentonite particles. For glass fibre-reinforced FaB mix samples, tensile resistance begins to develop within the fibres due to their interaction with coarse particles. The interlocking and interweaving of fibres with fly ash and bentonite particles contribute to intercepting the failure zones formed during testing. Furthermore, the irregular shape of fly ash particles enhances interlocking capacity, thereby contributing to the increase in UCS values.

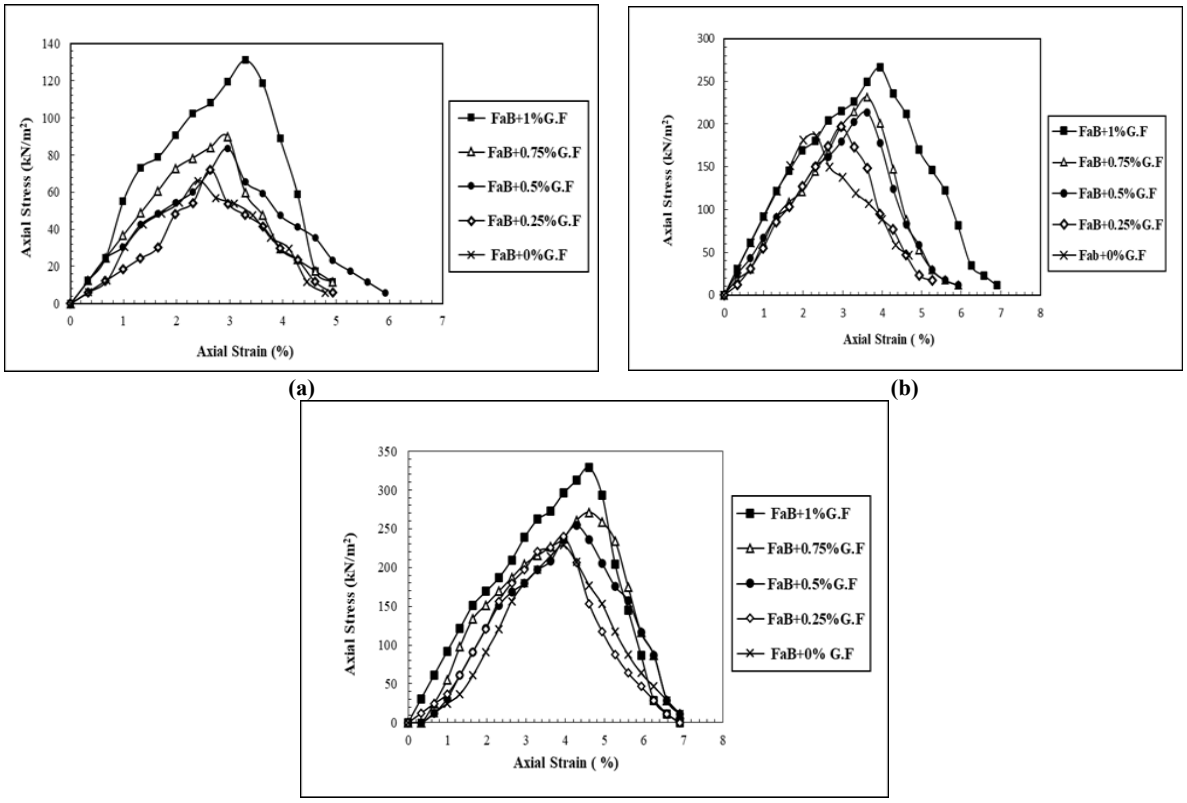

Figure 9. Axial stress – axial strain behavior of FaB mix samples with varying fibre content after (a) 7 days (b) 28 days and (c) 60 days of curing

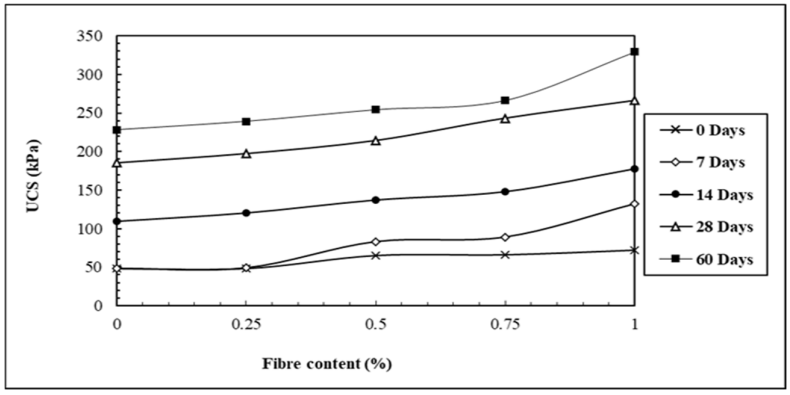

Figure 10. Variation of UCS with fibre content for varying curing periods

3.3. Compressibility Characteristics

3.3.1. Influence of Glass Fibre Content on Relationship of Void Ratio and Pressure

The fibre content plays a critical role in influencing the void ratio and the pressure response of FaB mixture. As illustrated in Figure 11, the void ratio versus logarithm of pressure (*e-log p*) plots for unreinforced and glass fibre-reinforced FaB mixtures reveal a consistent trend. The void ratio decreases with increasing pressure, which aligns with the typical compressibility behavior observed in soil and soil like geo-materials. However, the addition of fibres modifies this behavior significantly. An increase in fibre content results in higher void ratios under identical pressure conditions, which shows an enhancement in compressibility characteristics. This suggests that the addition of glass fibre reduces the overall compressibility of the FaB mixture and diminishes its tendency to compress under applied pressure. It is observed that the FaB+0%G.F mix sample exhibits the lowest void ratio and higher compressibility. The FaB+ 1%G.F sample maintains a comparatively higher void ratio which

enhances its resistance to compression. This resistance is attributed to the reinforcing mechanism introduced by the glass fibres, which improves the interparticle bonding and restricts unnecessary deformation. Consequently, fibre reinforcement contributes to a more stable and less compressible FaB mixture compared to its unreinforced counterpart.

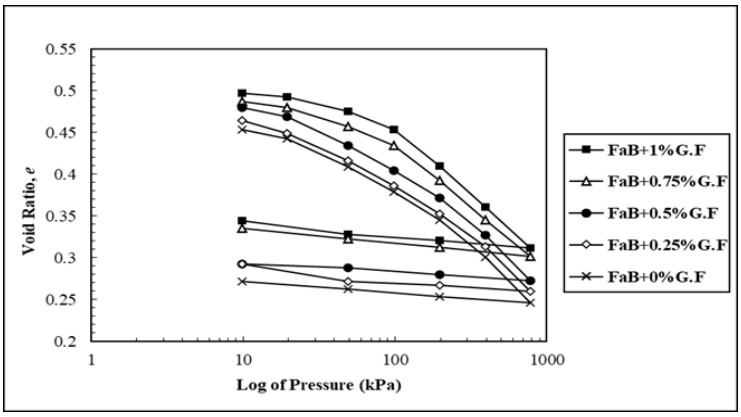

Figure 11. Void ratio to logarithm of Pressure (*e-log p*) plot for unreinforced and glass fibre-reinforced FaB mix samples

3.3.2. Influence of Glass Fibre Content on Compression Index (C_c)

The fibre content significantly influences the compression index (C_c) of FaB mixture, as shown in Figure 12. An increase in fibre content results in a decrease in C_c value, demonstrating the effectiveness of glass fibres in reducing the compressibility of FaB mixture. At FaB+0%G.F, the C_c value is relatively high i.e., 0.33. However, with the addition of fibres, there is a notable reduction in C_c for FaB+0.25%G.F mix sample. The most considerable decrease is observed at the fibre content of 0.25%, indicating that even a small quantity of glass fibre has a noticeable effect on compressibility. As fibre content continues to increase, the decline in C_c continues but at a more gradual rate.

The reduction in compressibility can be attributed to the reinforcing effect of the glass fibres within the FaB mixture, which enhances its overall strength and reduces the scope of deformation under applied pressure. The volumetric changes in the FaB mix samples result from mechanisms such as rolling, sliding, crushing, and bending of the coarser particles [77]. The mixing of glass fibres improve particle interlocking and binding within the mixture, leading to a more stable and less compressible structure. These fibres improve the structural integrity of the FaB mixture, and enhance its resistance to deformation under applied pressure.

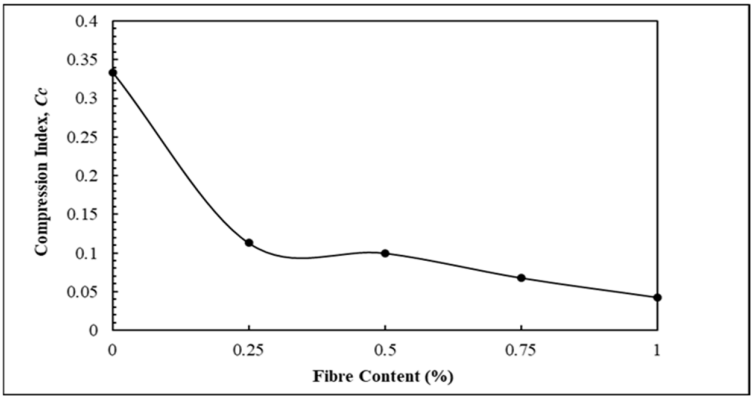

Figure 12. Influence of glass fibre content on compression index

3.3.3. Influence of Glass Fibre Content on Coefficient of Compressibility (a_v) and Coefficient of Volume Compressibility (m_v)

The coefficient of compressibility (a_v) indicates the compressibility behavior of a soil or soil-like material in terms of the rate of change in void ratio with respect to effective stress (Equation 1).

$$a_v = \frac{-\Delta e}{\Delta \bar{\sigma}} \quad (1)$$

Where;

a_v = coefficient of compressibility (m^2/kN)

$\Delta\bar{\sigma}$ = change in effective stress (kPa)

Δe = change in void ratio

Figure 13(a) shows the variation in a_v of the FaB mixture with different fibre contents. It is evident that a_v decreases as the fibre content increases. At 0% glass fibre content, the FaB mixture exhibits a high a_v value which shows greater compressibility in the unreinforced state. With the introduction of a small amount of glass fibre (0.25%), a sharp reduction in a_v is observed. This can be attributed to the reinforcing action of the glass fibres, which function as tensile elements within the FaB mixture. Under applied incremental loads, a load transfer mechanism has been initiated, wherein the applied stresses are distributed between the fly ash and bentonite particles. Additionally, the presence of fibres hinders particle rearrangement and sliding, thereby minimizing changes in void ratio. As the fibre content increases from 0.25% to 1%, a_v continues to decrease, although at a reduced rate. The glass fibres effectively bridge the voids and bind the fly ash and bentonite particles, resulting in a denser and less compressible mixture. The most significant reduction in a_v is observed for the FaB+0.75%G.F mix sample. Beyond this, further increments in fibre content do not significantly influence the coefficient of compressibility.

The coefficient of volume compressibility (m_v) is defined as volumetric strain per unit increase in effective stress (Equation 2).

$$m_v = \frac{a_v}{1 + e_0} \quad (2)$$

Where;

a_v = coefficient of compressibility (m^2/kN)

e_0 = initial void ratio

m_v = coefficient of volume compressibility (m^2/kN)

Figure 13(b) illustrates the variation of m_v with fibre content in the FaB mixture. The plot shows that m_v decreases as the fibre content increases. Since m_v is proportional to a_v, a similar trend is observed, as previously explained. This reduction in m_v can be attributed to the reinforcing effect of the glass fibres within the FaB mixture.

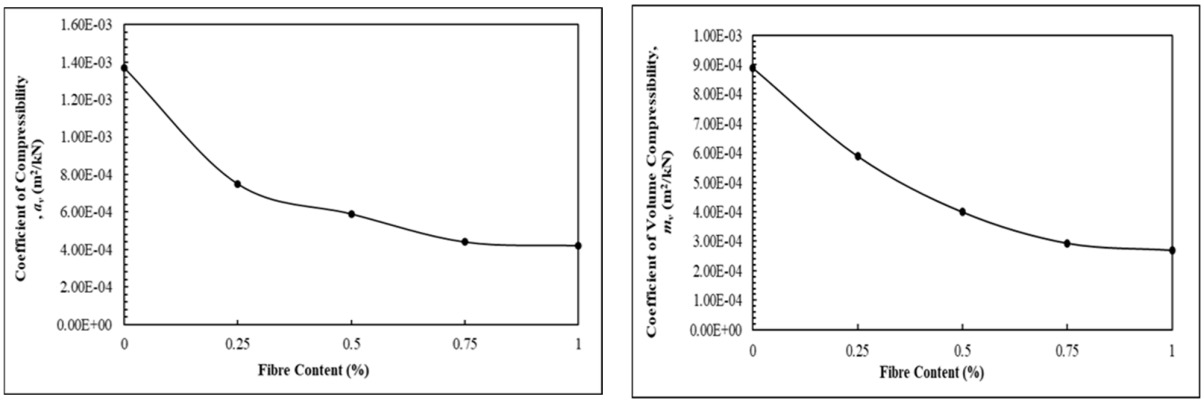

(a) (b)

Figure 13. Influence of glass fibre content on (a) coefficient of compressibility and (b) coefficient of volume compressibility

3.3.4. Influence of Glass Fibre Content on Coefficient of Permeability (k)

To observe the influence of varying fibre content on the coefficient of permeability (k), the value of k has been calculated using Equation (3).

$$k = c_v \times m_v \times \gamma_w \quad (3)$$

Where;

c_v = coefficient of consolidation (m^2/sec)

m_v = coefficient of volume compressibility (m^2/kN)

γ_w = unit weight of water (kN/m^3)

k = coefficient of permeability (m/sec)

Figure 14 shows the variation of the coefficient of permeability (k) with glass fibre content. It is evident that even a slight increase in glass fibre content leads to a significant decrease in the value of k. When the glass fibre content increases from 0% to 0.25%, there is a sharp drop in k from 1.8×10^{-8} m/sec to 9.09×10^{-9} m/sec. This initial reduction is mainly due to the reinforcing effect introduced by the glass fibre. The addition of glass fibre reduces the void ratio in the FaB mixture by enhancing the interlocking and bonding between the fly ash and bentonite particles. As a result, the reduced voids and pore spaces restrict water flow, leading to a considerable decrease in the coefficient of permeability (k) value for the fibre-reinforced FaB mixture. Beyond 0.25% glass fibre content, the value of k continues to decrease but at a gradual rate. As the increase in glass fibre content beyond 0.25% does not notably influence the compressibility of the FaB mixture, the rate of reduction in permeability decreases. The lowest value of k is observed for the FaB+1%G.F mix sample as 5.89×10^{-9} m/sec.

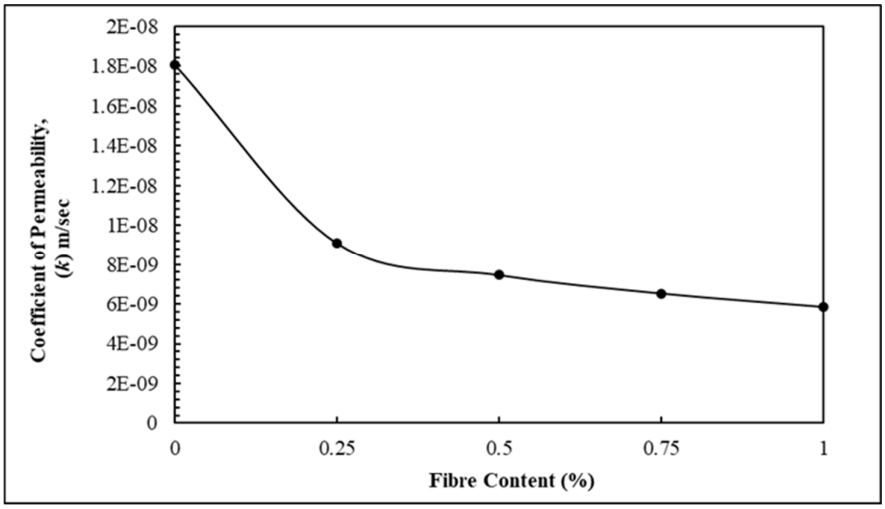

Figure 14. Influence of fibre content on coefficient of permeability

4. Predictive Model for UCS

Based on results obtained from extensive experimental investigations, this study proposed a closed-form equation for predicting the UCS value of 80:20 FaB mixture with and without glass fibre reinforcement. The proposed expression (Equation 4) is derived from data obtained through UCS testing and is formulated as a function of curing period (C_p), relative moisture content (R.M.C), and fibre content (f_c). This equation serves as a practical tool for engineers and practitioners to estimate the strength of glass fibre-reinforced FaB mixtures for specific curing periods, moisture, and fibre contents in advance of the construction stage. Figure 15 illustrates a comparison between the predicted and experimentally obtained UCS values, which are in close agreement with a variation within ±10%. The proposed equation yields a regression coefficient of 0.93, indicating a high level of reliability and predictive accuracy for UCS of both unreinforced and glass fibre-reinforced FaB mixtures.

$$UCS = 483.2815 + 54.016f_c + 5.94C_p - 428.797R.M.C - 0.00074{C_p}^3 - 13.47R.M.C^{-10} \quad (4)$$

Where:

UCS = Unconfined compressive strength of unreinforced and glass fibre-reinforced FaB mixture (kPa)

f_c = Fibre content (%)

C_p = Curing period (Days)

R.M.C = Relative Moisture Content

$$\text{R.M.C} = \frac{Molding\ moisture\ content\ of\ FAB\ mix\ sample(\%)}{Optimum\ moisture\ content\ of\ the\ respective\ sample(\%)}$$

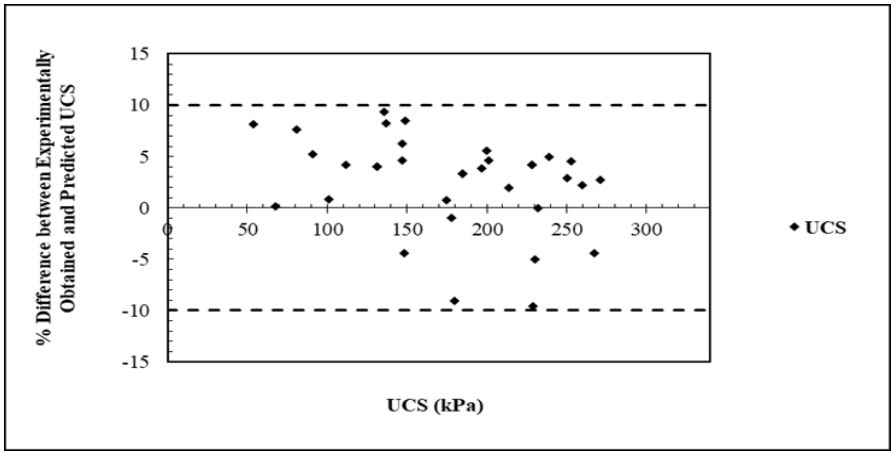

Figure 15. Comparison between experimentally observed and predicted UCS values

5. Conclusions

In the present study, the influence of glass fibre on the strength and permeability behavior has been studied. Based on the extensive experimental investigations, the following conclusions can be drawn:

- Influence of curing period on UCS: The UCS values increase with curing time for unreinforced and glass fibre-reinforced FaB mix samples. This enhancement is attributed to the gradual formation of cementitious compounds via pozzolanic reactions, which progressively fill voids and micro-cracks within the sample. This resulting densification leads to improvement of structural integrity and strength.
- Influence of R.M.C: As R.M.C increases from 80% to 90%, the UCS values also rise across all curing periods and reinforcement conditions. The increased moisture content enhances pozzolanic activity, facilitating better strength development. At 90% R.M.C, optimal lubrication occurs which promotes densification. Beyond 90% R.M.C, the UCS begins to decrease for both unreinforced and glass fibre-reinforced FaB mix samples likely due to the presence of excessive moisture that hinders particle bonding.
- Influence of fibre content on UCS: At all curing periods, UCS increases with the addition of glass fibres. The strength gain is primarily due to mechanical interactions between the fibres and the fly ash and bentonite particles. At OMC, 1% glass fibre addition leads to a UCS enhancement of approximately 33%-44% considering all curing periods. This improvement occurs due to the tensile reinforcement provided by the glass fibres.
- Influence of fibre content on compressibility: Increasing glass fibre content results in decreased compressibility. This is attributed to the reinforcing effect of glass fibres which enhances the interparticle bonding and promotes structural interlocking. Although C_c continues to decrease with the addition of glass fibre content, the rate of reduction slows beyond 0.25% fibre content. Both a_v and m_v exhibit a declining trend with increased glass fibre content. A notable reduction is observed with the addition of 0.25% glass fibre, due to the bridging and reinforcing effects.
- Influence of fibre content on permeability: The coefficient of permeability (k) decreases by an order of magnitude 10^{-1} with glass fibre addition. This is primarily due to the reduced void ratio in glass fibre-reinforced FaB mix samples. The glass fibres contribute to improve the interparticle bonding and matrix densification, which collectively restrict water flow and decrease permeability. The lowest value of k is observed for the FaB+1%G.F mix sample as 5.89×10^{-9} m/sec.
- Based on the experimentally obtained data, a closed-form equation has been developed to estimate the UCS of 80:20 FaB mixture with and without glass fibre reinforcement. This predictive model provides practitioners with a reliable tool to assess the strength during the pre-design phase of construction.

Finally, the addition of glass fibres into FaB mixture significantly enhances its strength, reduces

compressibility and coefficient of permeability. These improvements make glass fibre-reinforced FaB mixture a promising alternate geo-material. By facilitating increased utilization of fly ash and minimizing its disposal concerns, this innovation contributes to environmentally responsible construction practices.

List of Notations

C_p= Curing period

c_v = Coefficient of consolidation

e_0 = Initial void ratio

f_c= Fibre content in percentage

m_v = Coefficient of volume compressibility

γ_w = Unit weight of water

$\Delta\bar{\sigma}$ = Change in effective stress

Δe = Change in void ratio

C_c = Compression index

e = Void ratio

G = Specific gravity

k = Coefficient of permeability

a_v = Coefficient of compressibility

p = Pressure

List of Abbreviations

Fa = Fly ash

FaB = Fly ash- Bentonite

FaB+0%G.F = FaB sample reinforced with 0% glass fibre (unreinforced FaB mix samples)

FaB+0.25%G.F = FaB sample reinforced with 0.25% glass fibre

FaB+0.5%G.F = FaB sample reinforced with 0.5% glass fibre

FaB+0.75%G.F = FaB sample reinforced with 0.75% glass fibre

FaB+1%G.F = FaB mix samples reinforced with 1% glass fibre

G.F = Glass Fibre

MDD = Maximum Dry Density

OMC = Optimum Moisture Content

R.M.C = Relative Moisture Content

SEM = Scanning electron microscope

UCS = Unconfined Compressive Strength

Author contributions

All authors contributed to the study's conception. Material preparation and experiments have been performed by RK and AK. Manuscript writing and editing has been done by SC and RK. Supervision has been done by SC. All authors reviewed and approved the final draft.

Declarations

Conflict of Interest

The corresponding author certifies that I/we have no commercial associations (e.g., consultancies, stock ownership, equity interests, patent-licensing arrangements, etc.) that might pose a conflict of interest in connection with the submitted article, except as disclosed on a separate attachment. All funding sources supporting the work and all institutional or corporate affiliations of mine/ours are acknowledged in a footnote.

Human Participants and/or Animals

The authors declare that this article does not contain any studies involving animals and human participants performed by any of the authors.

Funding

No funding, grants, or other assistance have been obtained.

Data availability

Data will be provided upon request.

References

[1]. Alam, J., Khan, M. A., Alam, M. M., & Ahmad, A. (2012). Seepage characteristics and geotechnical properties of fly ash mixed with bentonite. *International Journal of Scientific Engineering Research, 3*(8), 1-11.

[2]. CEA (Central Electricity Authority) (2023). Fly ash generation at coal/lignite based thermal power stations and its utilization in the country. *CEA, New Delhi*.

[3]. Singh, S. P., & Sharan, A. (2014). Strength characteristics of compacted pond ash. *Geomechanics and Geoengineering, 9*(1), 9-17.

[4]. Rout, S., & Singh, S. P. (2020a). Characterization of pond ash-bentonite mixes as landfill liner material. *Waste Management & Research, 38*(12), 1420-1428.

[5]. Ram, A. K., & Mohanty, S. (2022). State of the art review on physiochemical and engineering characteristics of fly ash and its applications. *International Journal of Coal Science & Technology*, *9*(1), 9.

[6]. Nayak, D. K., Abhilash, P. P., Singh, R., Kumar, R., & Kumar, V. (2022). Fly ash for sustainable construction: A

review of fly ash concrete and its beneficial use case studies. *Cleaner Materials*, *6*, 100143.

[7]. Pradhip, V. P., Balu, S., & Subramanian, B. (2023). Pond ash as a potential material for sustainable geotechnical applications–a review. *Environmental Science and Pollution Research*, *30*(46), 102083-102103.

[8]. Sharma, S., & Vyas, A. K. (2024). Evaluation of mechanical properties of cement mortars containing pond ash as partial replacement of river sand and prediction of properties by regression models. *European Journal of Environmental and Civil Engineering*, *28*(11), 2679-2710.

[9]. Singh, C. K., & Kannari, L. D. (2024). Pond ash as a fine aggregate for controlled low-strength materials (CLSM): a study of its geotechnical and geoenvironmental aspects. *Multiscale and Multidisciplinary Modeling, Experiments and Design*, *7*(4), 3767-3781.

[10]. Nguyen, H. T., Nguyen, H. H., Nguyen, T. T. H., & Vu, Q. H. (2025). Experimental Study on Fly Ash-Cemented Soil for River Levee Overtopping Protection. *Geotechnical and Geological Engineering*, *43*(2), 109.

[11]. Kedar, H. N., & Patel, S. (2025). Optimization and characterization of lime and GGBS treated fly ash for sustainable road pavement applications. *Multiscale and Multidisciplinary Modeling, Experiments and Design*, *8*(1), 91.

[12]. Simatupang, M., Edwin, R. S., Sulha, S., Putra, H., & Yanto, D. H. Y. (2025). The evolution of the hydraulic conductivity of fly ash-treated sand as a liquefaction countermeasure. *Indian Geotechnical Journal*, *55*(1), 92-106.

[13]. Pani, A., & Singh, S. P. (2018). Effect of temperature on the strength of lime-stabilised fly ash. *Environmental Geotechnics*, *7*(3), 189-199.

[14]. Rout, S., & Singh, S. P. (2020b). Influence of fibers on hydro-mechanical properties of bentonitic mixtures. *Geotechnical and Geological Engineering*, *38*(3), 3145-3161.

[15]. Chowdhury, S., & Patra, N. R. (2021a). Experimental and numerical investigation on undrained behavior of geogrid reinforced pond ash. *Indian Geotechnical Journal*, *51*(6), 1182-1194.

[16]. Chowdhury, S., & Patra, N. R. (2021b). Settlement behavior of circular footing on geocell-and geogrid-reinforced pond ash bed under combine static and cyclic loading. *Arabian Journal of Geosciences*, *14*(11), 1063.

[17]. Chowdhury, S., & Patra, N. R. (2022). Undrained response of geocell-confined pond ash samples under static and cyclic loading. *Geosynthetics International*, *29*(3), 229-240.

[18]. Chowdhury, S., Roy, S., & Singh, S. P. (2023). Performance assessment of three alkali-treated fly ashes as a pavement base-course material. *Construction and Building Materials*, *365*, 130110.

[19]. Dandin, S., Kulkarni, M., & Wagale, M. (2023). Fly ash based subgrade reinforced with pet bottles as non-conventional geocell: a 3D finite element analysis. *Geotechnical and Geological Engineering*, *41*(2), 1537-1556.

[20]. Kedar, H. N., & Patel, S. (2024). Complete replacement of granular base layer with stabilized fly ash for road construction. *Indian Geotechnical Journal*, *54*(3), 1017-1031.

[21]. Pradhan, S. K., & Pothal, G. K. (2024). Experimental and cost evaluation of pond ash reinforced with polymeric geogrid. *Multiscale and Multidisciplinary Modeling, Experiments and Design*, *7*(1), 349-363.

[22]. Biswas, S., & Chowdhury, S. (2025). Prediction of Bearing Capacity of Closely Spaced Footings: Multilayer Geogrid-Reinforced Pond Ash Perspective. *International Journal of Geomechanics*, *25*(6), 04025087.

[23]. Fu, J., Wei, J., Haeri, H., Sarfarazi, V., Chehrepak, M. M., & Fatehi Marji, M. (2025). Investigation of Failure Mechanism of Geogrid Reinforced Porous Concrete Based on Experimental Test. *International Journal for Numerical and Analytical Methods in Geomechanics*, e70002.

[24]. Abharian, S., Sarfarazi, V., Marji, M. F., Rasekh, H., & Sadrekarimi, A. (2023). Effect of geogrid reinforcement on tensile failure of high-strength self-compacted concrete. *Magazine of Concrete Research*, *75*(8), 379-401

[25]. Nalbantoğlu, Z. (2004). Effectiveness of class C fly ash as an expansive soil stabilizer. *Construction and Building Materials*, *18*(6), 377-381.

[26]. Zha, F., Liu, S., Du, Y., & Cui, K. (2008). Behavior of expansive soils stabilized with fly ash. *Natural hazards*, *47*(3), 509-523.

[27]. Bose, B. (2012). Geo engineering properties of expansive soil stabilized with fly ash. *Electronic Journal of Geotechnical Engineering*, *17*(1), 1339-1353.

[28]. Kedar, H. N., Patel, S., & Shirol, S. S. (2024). Bulk utilization of steel slag–fly ash composite: a sustainable alternative for use as road construction materials. *Innovative Infrastructure Solutions*, *9*(1), 21.

[29]. Fan, R. D., Du, Y. J., Reddy, K. R., Liu, S. Y., & Yang, Y. L. (2014). Compressibility and hydraulic conductivity of clayey soil mixed with calcium bentonite for slurry wall backfill: Initial assessment. *Applied Clay Science*, *101*, 119-127.

[30]. Du, Y. J., Fan, R. D., Liu, S. Y., Reddy, K. R., & Jin, F. (2015). Workability, compressibility and hydraulic conductivity of zeolite-amended clayey soil/calcium-bentonite backfills for slurry-trench cutoff walls. *Engineering Geology*, *195*, 258-268.

[31]. Rout, S., & Singh, S. P. (2021). Prediction of compressibility and hydraulic conductivity of bentonitic mixtures. *Proceedings of the Institution of Civil Engineers-Geotechnical Engineering*, *174*(2), 225-237.

[32]. Subhadarsini, S., Giri, D., & Das, S. S. (2024). Parametric optimization of bentonite-fly-ash composite core for earthen embankment using Taguchi coupled sunflower optimization algorithm. *Innovative Infrastructure Solutions*, *9*(2), 43.

[33]. Gupt, C. B., Bordoloi, S., Sahoo, R. K., & Sekharan, S. (2021). Mechanical performance and micro-structure of bentonite-fly ash and bentonite-sand mixes for landfill liner application. *Journal of Cleaner Production*, *292*, 126033.

[34]. Kantesaria, N., Chandra, P., & Sachan, A. (2021, May). Geotechnical behaviour of fly ash-bentonite mixture as a liner material. In *Proceedings of the Indian Geotechnical Conference 2019: IGC-2019 volume II* (pp. 237-247). Singapore: Springer Singapore.

[35]. Rout, S., & Singh, S. P. (2023). Effect of compaction water on strength and hydraulic properties of bentonite-based liner. *Proceedings of the Institution of Civil Engineers-Geotechnical Engineering*, *177*(3), 291-302.

[36]. Kumar, R., Kanaujia, V. K., & Chandra, D. (1999). Engineering behaviour of fibre-reinforced pond ash and silty sand. *Geosynthetics International*, *6*(6), 509-518.

[37]. Hosseini, M., & Fakhri, D. (2021). Experimental study of effect of glass fibres on properties of concrete containing micro-silica and limestone powder. *Journal of Mining and Environment*, *12*(3), 895-906.

[38]. Boominathan, A., & Hari, S. (2002). Liquefaction strength of fly ash reinforced with randomly distributed fibers. *Soil Dynamics and Earthquake Engineering*, *22*(9-12), 1027-1033.

[39]. Ghosh, A., Ghosh, A., & Bera, A. K. (2005). Bearing capacity of square footing on pond ash reinforced with jute-geotextile. *Geotextiles and Geomembranes*, *23*(2), 144-173.

[40]. Fakhri, D., Hosseini, M., & Mahdikhani, M. (2022). Effect of glass and polypropylene hybrid fibers on Mode I, Mode II, and Mixed-Mode fracture toughness of concrete containing micro-silica and limestone powder. *Journal of Mining and Environment*, *13*(2), 559-577.

[41]. Das, A., Jayashree, C., & Viswanadham, B. V. S. (2009). Effect of randomly distributed geofibers on the piping behaviour of embankments constructed with fly ash as a fill material. *Geotextiles and Geomembranes*, *27*(5), 341-349.

[42]. Ghosh, A., & Dey, U. (2009). Bearing ratio of reinforced fly ash overlying soft soil and deformation modulus of fly ash. *Geotextiles and geomembranes*, *27*(4), 313-320.

[43]. Sreedhar, M. V. S., Reddy, Y. S., & Jyothi, A. (2011, December). CBR characteristics of pond ash with reinforcement in fabric and fibre forms. In *Indian Geotechnical Conference December* (pp. 15-17).

[44]. Kumar, D., & Sengupta, S. (2022). Liquefaction resistance of polypropylene strips reinforced sand-fly ash blend under strain-controlled cyclic triaxial test. *Innovative Infrastructure Solutions*, *7*(6), 355.

[45]. Tangirala, A., Rawat, S., & Lahoti, M. (2024). A year-long study of eco-friendly fibre reinforced cementitious composites with high volume fly ash and industrial waste aggregates. *Innovative Infrastructure Solutions*, *9*(5), 179.

[46]. Mishra, K., Behera, S. K., Patel, S. K., Singh, P., Buragohain, J., Hazra, B., & Kumar, R. (2024). Experimental Investigation on the Mechanical and Microstructural Properties of Cemented Coal Ash Based Paste Backfill Reinforced with Polypropylene Fibre. *Indian Geotechnical Journal*, 1-15.

[47]. Sun, L., Fu, J., Wang, D., Haeri, H., Guo, C. L., & Cheng, H. (2024). Investigating the effect of various fibers on plasticity and compressive strength of concrete samples. *Strength of Materials*, *56*(1), 200-208.

[48]. Fu, J., Sarfarazi, V., Haeri, H., Wang, Z., & Fatehi Marji, M. (2025). Improving the tensile strength of reinforced concrete: evaluating the impact of different fiber additives through numerical and experimental analysis. *Computational Particle Mechanics*, *12*(1), 775-792.

[49]. Maher, M. H., & Gray, D. H. (1990). Static response of sands reinforced with randomly distributed fibers. *Journal of geotechnical engineering*, *116*(11), 1661-1677.

[50]. Fatani, M. N., Bauer, G. E., & Al-Joulani, N. (1991). Reinforcing soil with aligned and randomly oriented metallic fibers. *Geotechnical Testing Journal*, *14*(1), 78-87.

[51]. Maher, M. H., & Ho, Y. C. (1993). Behavior of fiber-reinforced cemented sand under static and cyclic loads. *Geotechnical Testing Journal*, *16*(3), 330-338.

[52]. Ranjan, G., Vasan, R. M., & Charan, H. D. (1996). Probabilistic analysis of randomly distributed fiber-reinforced soil. *Journal of geotechnical engineering*, *122*(6), 419-426.

[53]. Diambra, A., & Ibraim, E. (2015). Fibre-reinforced sand: interaction at the fibre and grain scale. *Géotechnique*, *65*(4), 296-308.

[54]. Mukherjee, K., & Mishra, A. K. (2019a). Evaluation of hydraulic and strength characteristics of sand-bentonite mixtures with added tire fiber for landfill application. *Journal of Environmental Engineering*, *145*(6), 04019026.

[55]. Mukherjee, K., & Mishra, A. K. (2019b). Hydro-mechanical properties of sand-bentonite-glass fiber composite for landfill application. *KSCE Journal of Civil Engineering*, *23*(11), 4631-4640.

[56]. Mukherjee, K., & Mishra, A. K. (2020). Undrained performance of sustainable compacted sand-bentonite–glass fiber composite for landfill application. *Journal of Cleaner Production*, *244*, 118662.

[57]. Karki, B., & Kolay, P. K. (2024). Modification of bentonite clay using recycled glass powder and polypropylene fiber. *Geotechnical and Geological Engineering*, *42*(6), 5051-5064.

[58]. Deka, A., Gupt, C. B., & Sekharan, S. (2021). Analysis of WRCC of fly ash-bentonite mixes based on combined shrinkage and suction measurement. *Geotechnical and Geological Engineering*, *39*(5), 3889-3901.

[59]. Kumar, R., & Kumari, S. (2024a). A feasibility study of fly ash and bentonite composite mix for assessing its suitability as landfill liner material. *Sādhanā*, *49*(2), 98.

[60]. Kumar, R., & Kumari, S. (2024b). Exploring the geotechnical and microstructural properties of composite mixtures for landfill liner materials: an experimental investigation. *Environmental Science and Pollution Research*, *31*(22), 33011-33029.

[61]. Mukherjee, K., & Mishra, A. K. (2021). Impact of glass fibre on hydromechanical behaviour of compacted sand–bentonite mixture for landfill application. *European Journal of Environmental and Civil Engineering*, *25*(7), 1179-1200.

[62]. Mukherjee, K., & Mishra, A. K. (2022). An assessment of the mechanical performance of a novel sand bentonite-glass fiber composite for the avoidance of catastrophic landfill failure. *Construction and Building Materials*, *348*, 128644.

[63]. Rout, S., & Singh, S. P. (2017). Assessing the suitability of compacted bentonite-pond ash mixes as landfill liner. In *International Congress and Exhibition" Sustainable Civil Infrastructures: Innovative Infrastructure Geotechnology"* (pp. 314-327). Cham: Springer International Publishing.

[64]. Kumar, R., Gupta, L., Kumar, A., Kumar, S., Aslam, M., & Gupta, A. K. (2024). Abrasion resistance of glass fiber silica fume concrete. *Multiscale and Multidisciplinary Modeling, Experiments and Design*, *7*(6), 5149-5169.

[65]. Yaswanth, K. K., Vani, V. S., Biswal, K., Kumar, G. P., Manjula, C., Govindarajan, S., Bhavani, G.P & Prameela, U. (2025). A critical analysis of compressive strength prediction of glass fiber and carbon fiber reinforced concrete over machine learning models. *Multiscale and Multidisciplinary Modeling, Experiments and Design*, *8*(3), 178.

[66]. IS 2720 (Part-III) 1980. Methods of test for soils: Part 3 Determination of specific gravity, fine, medium and coarse-grained soils. India: Bureau of Indian Standards.

[67]. IS: 2720 (Part-IV)-1975 (Reaffirmed 2006): Methods of test for soils: Part 4 Grain size analysis. India: Bureau of Indian Standards.

[68]. IS: 2720 (Part-V)-1985 (Reaffirmed 2006): Methods of Test for Soils: Part 5 Determination of Liquid and Plastic Limit. India: Bureau of Indian Standards.

[69]. IS 2720 (Part-XII) 1980 (Reaffirmed 2011): Methods of test for soils: Part 7 Determination of water content-dry density relation using light compaction. India: Bureau of Indian Standards.

[70]. IS: 2720 (Part-X)-1991 (Reaffirmed 2010): Methods of Test for Soils: Part 10 Determination of Unconfined Compressive Strength. India: Bureau of Indian Standards.

[71]. Haeri, H., Khaloo, A. R., Shahriar, K., Fatehi Marji, M., & Moaref Vand, P. (2015). A boundary element analysis of crack-propagation mechanism of micro-cracks in rock-like specimens under a uniform normal tension. *Journal of Mining and Environment*, *6*(1), 73-93.

[72]. Haeri, H. (2015). Simulating the crack propagation mechanism of pre-cracked concrete specimens under shear loading conditions. *Strength of Materials*, *47*(4), 618-632.

[73]. Haeri, H. (2015). Erratum to: "Propagation mechanism of neighboring cracks in rock-like cylindrical specimens under uniaxial compression". *Journal of Mining Science*, *51*(5), 1062-1062.

[74]. Haeri, H. (2015). Experimental crack analyses of concrete-like CSCBD specimens using a higher order DDM. *Computers and Concrete, An International Journal*, *16*(6), 881-896.

[75]. Sarfarazi, V., Haeri, H., & Shemirani, A. B. (2017). Direct and indirect methods for determination of mode I fracture toughness using PFC2D. *Computers and Concrete, An International Journal*, *20*(1), 39-47. DOI:10.12989/cac.2017.20.1.039

[76]. IS: 2720 (Part-XV)-1986 (Reaffirmed 2002): Methods of Test for Soils: Part 15 Determination of Consolidation properties. India: Bureau of Indian Standards.

[77]. Mitchell, J. K., & Soga, K. (2005). Fundamentals of soil behavior. Virginia Tech University, Blacksburg, Virginia, USA.

انجمن مهندسی معدن ایران
نشریه مهندسی معدن و محیط زیست
نشانی نشریه: www.jme.shahroodut.ac.ir
دانشگاه صنعتی شاهرود

ارزیابی رفتار مقاومتی و نفوذپذیری مخلوط خاکستر بادی-بنتونیت تقویت‌شده با الیاف شیشه

سواراج چودهوری*، راکش کومار و انکیت کومار

گروه مهندسی عمران، موسسه ملی فناوری همیرپور، هیماچال پرادش - ۱۷۷۰۰۵، هند

اطلاعات مقاله

تاریخ ارسال: ۲۰۲۵/۰۷/۲۷
تاریخ داوری: ۲۰۲۵/۰۸/۲۸
تاریخ پذیرش: ۲۰۲۵/۰۹/۰۷

DOI:10.22044/jme.2025.16576.3242

کلمات کلیدی

برنامه ریزی تولید بلند مدت
برنامه ریزی ریاضی
پله های فعال
برنامه های عملیاتی
جابجایی تجهیزات

چکیده

مطالعه حاضر به بررسی رفتار مقاومتی و نفوذپذیری مخلوط خاکستر بادی-بنتونیت (FaB) تقویت‌شده با الیاف شیشه می‌پردازد تا پتانسیل آن را به عنوان یک مصالح ژئوتکنیکی جایگزین ارزیابی کند. مخلوط FaB با افزودن ۲۰٪ بنتونیت به همراه ۸۰٪ خاکستر بادی تولید شده و سپس با الیاف شیشه تقویت می‌شود. آزمایش‌های مقاومت فشاری تک‌محوری (UCS) با نرخ کرنش ۰.۶۲۵ میلی‌متر بر دقیقه با تغییر دوره عمل‌آوری (۰ تا ۶۰ روز)، رطوبت نسبی (۸۰٪ RMC - ۱۲۰٪ تا) و محتوای الیاف (۰٪ تا ۱.۰٪) انجام شده است. تأثیر محتوای الیاف بر ضریب نفوذپذیری (k) و رفتار تراکم‌پذیری مخلوط FaB از طریق آزمایش‌های تحکیم یک بعدی بررسی شده است. یافته‌ها نشان می‌دهد که UCS نمونه‌های مخلوط FaB با افزایش دوره عمل‌آوری و محتوای الیاف بهبود می‌یابد. در ۱۰۰٪ R.M.C، با افزایش دوره عمل‌آوری از ۰ به ۶۰ روز، UCS برای نمونه‌های غیرمسلح از ۴۸ کیلوپاسکال به ۲۲۸ کیلوپاسکال افزایش می‌یابد. در ۹۰٪ R.M.C، هر دو نمونه مخلوط FaB تقویت نشده و تقویت شده، بالاترین مقادیر UCS را با توجه به تمام دوره‌های عمل‌آوری نشان داده‌اند. با افزایش محتوای الیاف از ۰٪ به ۱.۰٪، UCS در ۱۰۰٪ R.M.C حدود ۳۳٪ به ۴۴٪ افزایش می‌یابد. تقویت الیاف همچنین به کاهش k و تراکم‌پذیری کمک می‌کند. بر اساس یافته‌های تجربی، یک معادله بسته برای پیش‌بینی UCS مخلوط FaB تقویت‌شده با و بدون الیاف شیشه توسعه داده شده است. نتایج تأیید می‌کند که تقویت الیاف شیشه، مقاومت، نفوذپذیری و تراکم‌پذیری مخلوط FaB را بهبود می‌بخشد و آن را به عنوان یک ژئومتریال جایگزین معرفی می‌کند.

نویسنده مسئول مکاتبات: swaraj@nith.ac.in (س. چودهوری)